Evidence of slow millennial cliff retreat rates using cosmogenic nuclides in coastal colluvium

Rémi Bossis[1,2], Vincent Regard[1], Sébastien Carretier[1], and Sandrine Choy[1]

[1]GET, Université de Toulouse, CNES, CNRS, IRD, UPS, (Toulouse) France
[2]CEREGE, Université de Aix-Marseille, IRD, CNRS, Collège de France, Aix en Provence, France

Correspondence: Vincent Regard (vincent.regard@get.omp.eu) and Sébastien Carretier (sebastien.carretier@get.omp.eu)

Abstract. The erosion of rocky coasts contributes to global cycles of elements over geological times and also constitutes a major hazard that may potentially increase in the future. Yet, it remains a challenge to quantify rocky coast retreat rates over millennia; a time span that encompasses the stochasticity of the processes involved. Specifically, there are no available methods that can be used to quantify slow coastal erosion (< 1cm yr^{-1}) averaged over millennia. Here, we use the ^{10}Be concentration in colluvium, corresponding to the by-product of aerial rocky coast erosion, to quantify the local coastal retreat rate averaged over millennia. We test this approach along the Mediterranean coast of the Eastern Pyrenees (n=8) and the desert coast in Southern Peru (n=3). We observe a consistent relationship between the inferred erosion rates and the geomorphic contexts. The retreat rates are similar, 0.3-0.6 mm yr^{-1} for five samples taken on the Mediterranean coast, whereas two samples from vegetated colluvium have a lower rate of $\sim$0.1 mm yr^{-1}. The coastal retreat rate of the Peruvian site currently subject to wave action is similar to the Mediterranean coast (0.5 mm yr^{-1}), despite Peru's more arid climate. The other two Peruvian sites, which have not been subjected to wave action for tens of thousands of years, are eroding twenty times more slowly. Although the integration periods of the two slowest Mediterranean coast erosion rates may encompass pre-Holocene times, during which the sea-level and thus the retreat rate were much lower, we conclude here that the associated bias on the inferred retreat rate is less than 80%. These data show that rocky coasts are eroding 1 to 20 times faster than catchments in the same regions on average over the last few thousand years. We anticipate that this new method of quantifying slow rocky coastal erosion will fill a major gap in the coastal erosion database and improve our understanding of both coastal erosion factors and hazards.

1 Introduction

Rocky coasts, which represent approximately 50% of the world's coastline (Young and Carilli, 2019; Regard et al., 2022), are eroding by wave action (Sunamura, 1992; Trenhaile, 2002) through processes not fully understood yet (Prémaillon et al., 2018). Coastal erosion likely contributes to global cycles of elements (Regard et al., 2022) and also constitutes a hazard with implications for infrastructures and economy that is possibly amplified by global climate change (e.g. Ashton et al., 2011). Both aspects require documentation of coastal cliff erosion over different time spans, including millennial timescales; something that remains a challenge today. Coastal erosion occurs irregularly and varies over several time scales: daily depending on wave energy (tide), annually depending on the frequency and intensity of storms, over decadal to centennial periods because

of rising sea levels linked to climate change, and over multi-millennial periods depending on relative see level changes. Land-slides can also affect coastal erosion and participate to the stochastic nature of the retreat over decadal to centennial time spans (Prémaillon et al., 2018). Thus, there is currently a growing effort to quantify the erosion rates of rocky coasts (Prémaillon et al., 2018). The two most commonly used methods are the comparison of aerial photos (e.g. Dornbusch et al., 2008; Hapke et al., 2009; Letortu et al., 2014) and, for the past fifteen years, the comparison of 3D point clouds collected by photogrammetry or lidar (cf. Rosser et al., 2013; Dewez et al., 2013; Prémaillon et al., 2021; Swirad and Young, 2022). Lidar offers very good resolution but its maximum time span does not integrate all the stochastic nature of erosion, which in some cases is achieved by collapses with a long (>100 yrs) return time (Dewez et al., 2013; Dornbusch et al., 2008). Aerial photography can increase the temporal range to more than 50 years (Letortu et al., 2014; Dornbusch et al., 2008) but is then limited by the resolution and therefore, this technique is ineffective for capturing low retreat rates.

The lack of a reliable method to document millennial rates has led to the development of retreat rate measurements based on the concentration of cosmogenic isotopes in rocks from the shore platform (Choi et al., 2012; Regard et al., 2012; Rogers et al., 2012). These measurements have proven effective in quantifying millennial velocities between 10 and 300 mm/a, but require accurate measurements of the platform shape (Regard et al., 2012; Hurst et al., 2016; Swirad et al., 2020; Duguet et al., 2021; Shadrick et al., 2021; Clow et al., 2023). In addition, such a measurement has never been attempted on rocks more resistant to waves action for which shore platforms are narrower with complex geometry, limiting the possibility to evidence slow coastal retreat rates. Given that the available methods are adapted for rapid retreat rates, it is possible that the current database of rocky coast erosion rates is biased towards these rapid values (Prémaillon et al., 2018). As a result, complementary methods are much needed.

In this work, we introduce a new method for quantifying millennial cliff retreat by analyzing cosmogenic isotopes in col-luvium. Cosmogenic isotopes have already been used to quantify the erosion of escarpments, either from river sediments to derive an average erosion rate for the catchment draining the escarpment (e.g. Wang and Willett, 2021; Stokes et al., 2023), or from local sampling of outcropping bedrock (e.g. Cockburn et al., 2000; Heimsath et al., 2006). The main difference with these previous methods is that the method developed here applies to a coastal scarp, and that this scarp is not dissected by rivers. This method is derived from a method that is already being implemented to measure the retreat rate of alluvial valley sides (Zavala et al., 2021). With this method, we obtain slow cliff retreat rates, between 0.05 and 0.5 mm/a. The integration time of this method is of the order of the inverse of the retreat rate, namely between 2 and 20 kyrs. These periods are longer than the rarest storms and collapses and therefore average out the stochastic phenomena. We therefore believe that this approach can provide a new tool for quantifying the erosion of rocky coastlines over these time periods.
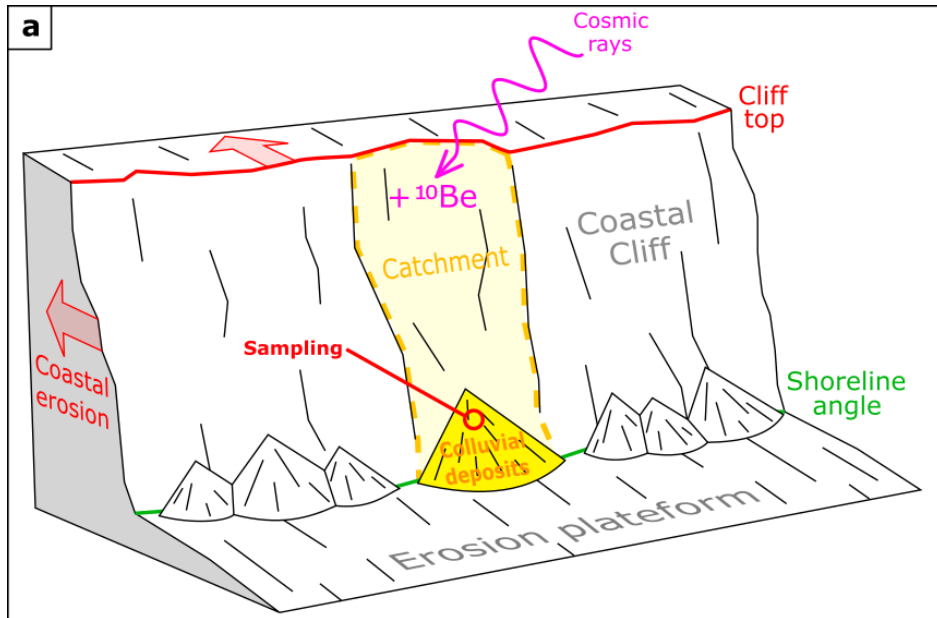
Figure 1. a: Shore platform/retreating cliff sketch showing the sampling strategy on colluviums at the foot of a coastal cliff. The sampled colluviums are active, suggesting that the erosion of the cliff is ongoing. b: View from the southwest of the coastal cliff at the BRAV3 site. The cliff is 80-100 m high. c: Sampling of one of the colluvium samples at the BRAV3 site. d: Sampling close-up view: the finest part of the grains is sampled until reaching roughly 1 kg of grains from several colluvium samples.

2 Method and sampling

The proposed method is based on the assumption that 1 kg of colluvium sampled at the foot of a rocky coast includes grains detached all along the coastal scarp above it (Figure 1). The sampled colluvial wedge is active, indicating ongoing erosion of the cliff. The mean ^{10}Be concentration of this colluvium sample can be converted into the mean erosion rate of the rocky coast, assuming a secular steady state in this concentration. This principle is nothing more than one of the assumptions that underlines the widely used method using ^{10}Be in river sands to quantify the average erosion rate of catchments (von Blanckenburg, 2005).

Each study site is composed of a shore erosion platform backed by a retreating cliff (Figure 2, see Supplementary for complete site descriptions). The cliff or escarpment face has a roughly constant slope. The erosion of the cliff produces colluvium that lies at its base. Three criteria were used to select the sampling sites: (i) the lithology must guarantee the presence of quartz grains in the colluvium; (ii) the geomorphological context must limit, as much as possible, the contribution of sediment coming from the areas above the cliff, which allows to constrain the source of the colluvium. To do this, we selected portions of the coast where cliff top also corresponds to a drainage divide, or which are located at the front of ridges between two rivers. In the latter case, the probability of a grain coming from above the linear face of the escarpment is minimal; (iii) lastly, it must be possible to access the foot of the cliffs in order to carry out the sampling.

The studied escarpments are a few dozen metres high on the Pyrenean coast and a few hundred metres high in Peru. The cliff surface is covered by a regolith in Peru, and in the Pyrenean coast a fine regolith alternates with outcroping bedrock. Sampling was conducted using the method described in Zavala et al. (2021). For each sampling site, about five colluvium samples were collected at the surface of debris wedges along a 50 m stretch of the cliff and then mixed together to obtain approximately 1 kilogram of material (Figure 1). This protocol was implemented so that our sampling was as representative as possible of sediment sources of coastal escarpment at each site. We took care to avoid sampling sediment that might have been deep in colluvium before being excavated very recently. Two examples of this care when sampling: in Peru, along the coastal road, above the road cut (Supplementary Figure S23), or at the foot of the coastal escarpment, we sampled colluvium above the area eroded by the sea (Supplementary Figures S2-S24). To do this, we systematically sampled debris wedges that covered any slope break at the toe of the escarpment (located usually a few metres above the sea), so that the sediment sampled necessarily came from higher up (i.e., no contamination by sand brought in by waves). In most cases, the debris wedges are located at the outlets of shallow debris channels eroding the escarpment, which increases the likelihood that the sediment collected statistically come from the entire escarpment (Supplementary Figure S2-S24). We also collected sediment a few metres above sea level to avoid

85   any contribution from pelagic sand.

     The 0.5-1 mm sand fraction was then chemically prepared following the protocol described in Zavala et al. (2021). The C concentration in [10]Be was then measured at AMS ASTER (CEREGE, Aix-en-Provence, France).

90   To calculate the average [10]Be production rate, we first determined a polygon bounded downstream by the sampling line and upstream by the cliff crest line, which also constitutes a limit for sediment sources. The average production rate (Table 1) was then calculated by averaging its value over all the pixels of the Digital Elevation Models (DEMs, Figure 2) contained within this polygon. The French airborne Lidar-derived RGE ALTI5 DEM with 5 m resolution was used for France (https://geoservices.ign.fr/) and the SRTM DEM (about 30 m of resolution) was used for Peru (https://www.earthdata.nasa.gov/).
95   For each pixel, the [10]Be production rate is determined by:

$$P = P_{sp} + P_{sm} + P_{fm} \tag{1}$$
$$P_{sp} = P_{SLHL} f_{sp} S_{sp} \tag{2}$$
$$P_{sm} = P_{SLHL} f_{sm} S_{sm} \tag{3}$$
$$P_{fm} = P_{SLHL} f_{fm} S_{fm} \tag{4}$$

100   where P_{sp}, P_{sm} and P_{fm} are the [10]Be production rates of a given CN at the Earth's surface by spallation (subscript "sp"), slow muon capture (subscript "sm") and fast muon interactions (subscript "fm"), respectively (Braucher et al., 2003). P_{SLHL} is the total sea-level/high-latitude production rate of the considered nuclide ($P_{SLHL} = 4$ atoms g^{-1} yr^{-1}). f_{sp}, f_{sm} and f_{fm} are the fractions of this production rate due to spallation, slow muon capture and fast muon interactions ($f_{sp} = 0.9886$, $f_{sm} = 0.0027$, $f_{fm} = 0.0087$). S_{sp}, S_{sm}, and S_{fm} are the respective scaling factors depending on latitude and elevation based on
105   Stone (2000).

     P can be decreased by topographic shielding and increased by the shorter cosmic ray distance between the scarp surface and any given point inside the rock on steep slopes (DiBiase, 2018). In order to evaluate the factor that should multiply P, we used the Matlab code provided by DiBiase (2018) and we computed this factor for different scarp slopes between 20 and 85
110   degrees corresponding to the range of our sites. We found that the factor increases slightly from 1.0006 for 20 degrees to 1.107 for 60 degrees, and then sharply from 1.17 for 65 degrees to 3.1 for 85 degrees. The factor is always greater than 1 because the effect of shorter cosmic ray paths dominates over the topographic shielding, as explained by DiBiase (2018). We corrected all the [10]Be production rates calculated in the following by this factor, which remain on the order of 1.1 as the slopes are smaller than 60 degrees.

115

The mean erosion rate ϵ was calculated assuming steady-state and neglecting the radioactive decay:

$$\epsilon \quad = \quad \frac{1}{\rho C}(P_{sp}\Lambda_{sp} + P_{sm}\Lambda_{sm} + P_{fm}\Lambda_{fm}) \tag{5}$$

where C is the sample ^{10}Be concentration and the rock density $\rho = 2.6$ g cm^{-3}. Neglecting radioactive decay is justified here because the estimated integration times are much shorter than the ^{10}Be half-life.

120

The erosion rate uncertainty corresponds to the propagated analytical uncertainty and the 15% uncertainty on P. Using the neutron attenuation length $L = \Lambda_{sp}/\rho$ of 0.6 m, we calculated the integration time $\tau = \frac{L}{\epsilon}$ for each sampled cliff (Table 1).

For catchments with a strong 3D curvature including an escarpment, Wang and Willett (2021) proposed a method for quan-
125 tifying the horizontal retreat of the escarpment by considering that the flux of eroded material occurred through a vertical surface. In our case, the escarpments have an almost constant slope α. Thus, we simply turn ϵ into a horizontal cliff retreat rate $r = \frac{\epsilon}{tan(\alpha)}$. In the following examples, r is similar to ϵ because the slopes of the cliffs are all close to $\alpha = 45°$ (Table 1).

As no other method exists to validate our approach, we tested its consistency by comparing our results with the geomorphic
130 context. Three study areas were sampled: the Côte Vermeille in southern France, close to the Spanish border, to the north of Banyuls-sur-Mer (samples VERM, Figure 2a); the Costa Brava coast around Sant Feliu de Guixols and Tossa de Mar in Spain (samples BRAV, Figure 2b); and around Atico in the Peru coastal desert (COSTA samples, Figure 2c).

The cliffs of the VERM series are 15 to 40 m high and consist of pelites and sandstone-pelites ("Argelès-sur-Mer" geologic
135 map, 1:50000, French Bureau de Recherches Géologiques et Minières; "Llançà" geologic map, 1:50000, Institut Cartogràfic i Geològic de Catalunya). The colluvium of the VERM1 and VERM2 sites are relatively fresh while those of the VERM3 site appear older because they are partly stabilized by herbaceous plants (it can be estimated that this vegetation needs a decade to become established).

The cliffs of the BRAV series are 50 to 120 m high and consist of leucogranites (BRAV1, BRAV2, BRAV3 and BRAV4)
140 and granodiorites and alkaline granites (BRAV5; "Baix Empordà" and "Selva" geologic maps, 1:50000, Institut Cartogràfic i Geològic de Catalunya). The colluvial wedges of the BRAV1, BRAV2, BRAV3 and BRAV4 sites are relatively fresh, while those of the BRAV5 site are largely stabilized by abundant vegetation consisting of trees. BRAV2 is the only sample for which part of the sampled sand could come from above the coastal escarpment. We discuss this further below. In this area, sea level
145 rose rapidly just after the last glacial maximum, and then at a decreasing rate, to reach a more or less constant rise of around 0.4 mm/year over the last six millennia (Vacchi et al., 2021).

The sample sites for the COSTA series were selected to test the effect of a drier climate. Furthermore, some parts of the coast have been protected from the action of waves by the uplift of a shore platform related to the subduction of the Nazca plate
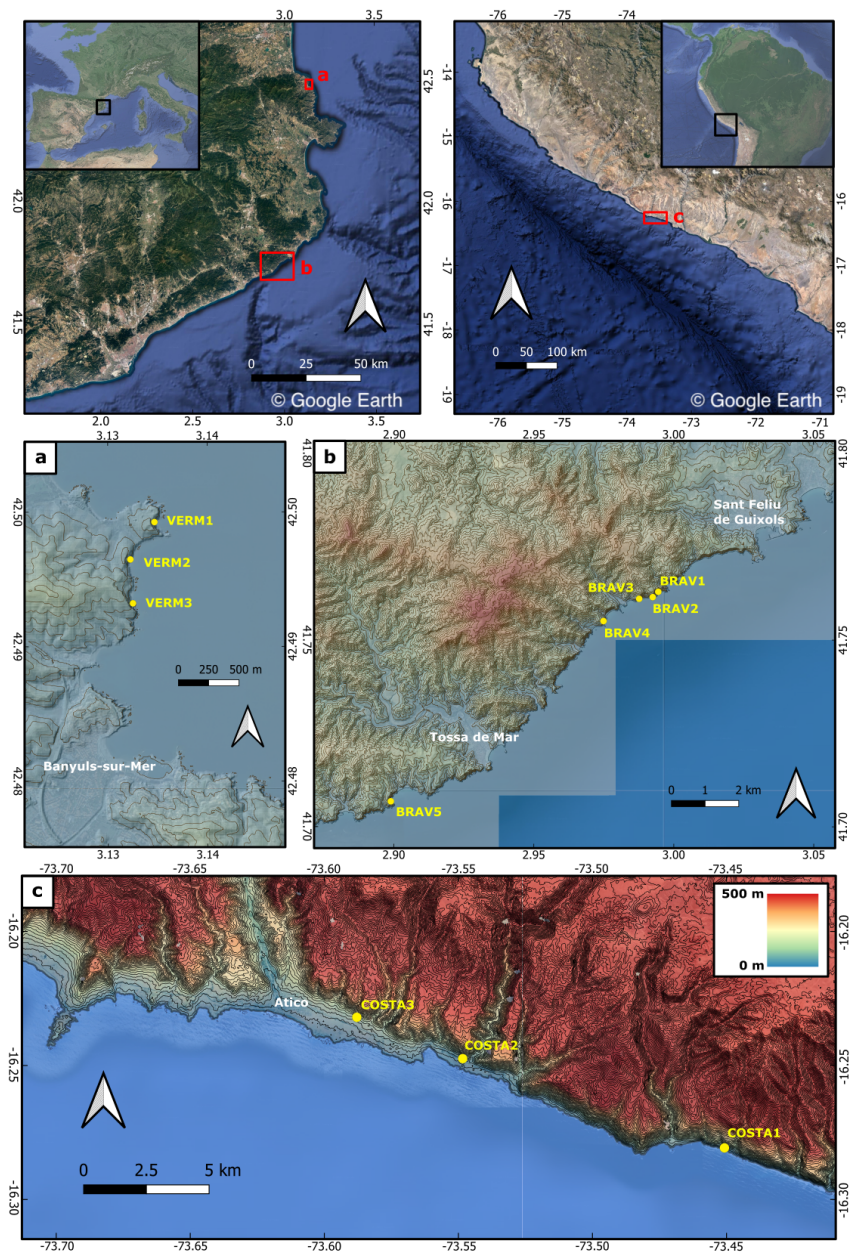
Figure 2. Sampling sites of this study. Top: general location of the series of sampled cliffs (Mediterranean Eastern Pyrenees on the left and Southern Peru on the right) using Google Earth views. a: Location of the VERM series samples on the 5 m horizontal resolution DEM (French Institut Géographique National). b: Location of the BRAV series samples on the 5 m horizontal resolution DEM (Institut Cartogràfic i Geològic de Catalunya). c: Location of the COSTA series samples on the 30 m horizontal resolution DEM (SRTM1). Note the presence of the uplifted platform at the foot of the cliff for COSTA2 and COSTA3. Contour lines are traced every 20 m in all topographic maps.

beneath South America at a rate of about 0.45 mm yr^{-1} over the Pleistocene (cf. Regard et al., 2021, 2010; Melnick, 2016; Malatesta et al., 2022; Saillard et al., 2017). The emergence of such a platform at the base of the cliff stops direct wave action at the bottom of the cliff (emergence since 200 ka after cliff foot elevation). Erosion rates measured on these cliffs should therefore be lower than those measured on active cliffs. COSTA1 was sampled at the base of an active cliff, whereas COSTA2 and COSTA3 were sampled over an uplifted shore platform spanning approximately 300 m and 1 km wide, respectively (Figure 2c). The cliffs are between 200 and 300 m high and are made of intrusive rocks (coastal batholith). The arid climate prevents the development of vegetation on these colluvial wedges.

3   Results

Table 1 and Figure 3 show the obtained erosion rates, similar to the retreat rates, and their respective integration times. For the VERM and COSTA series, five samples yield similar low erosion rates between 0.3 and 0.6 mm yr^{-1}. Two other samples (VERM3 and BRAV5), gathered from vegetated colluvium, have consistently lower rates between 0.05 and 0.1 mm yr^{-1}. An erosion rate similar to VERM and COSTA active sites is obtained for the COSTA1 sample in arid Peru, subject to wave erosion. The COSTA2 and COSTA3 samples, gathered on a paleo-cliff protected from wave action, are eroding $\sim$20 times more slowly (Table 1, Figure 3). The integration times range from 1.1 to 33.6 kyrs (Table 1, Figure 3), i.e. from late Holocene to pre-LGM periods.

Table 1. Features and results for each sample. The mean slope α (°) of the cliff was measured in the field. The mean production rate P (at/g yr^{-1}) of cosmogenic ^{10}Be was calculated for the (narrow) catchment upstream each sampling site using the DEMs of each location; it includes a correction for the slope following DiBiase (2018) (cf. text). The vertical erosion rate ϵ (mm yr^{-1}) was calculated from the concentration C in ^{10}Be with a neutron attenuation length L of 0.6 m and assuming 15% of uncertainty on P. The horizontal retreat rate r (mm yr^{-1}) was calculated from α, ϵ and propagating the uncertainty on ϵ. The integration time τ (yr) was calculated from L and ϵ (see text and Supplementary Material for more details).

Sample	latitude	longitude	[^{10}Be]	α	P	ϵ	r	τ
	°N	°E	at g^{-1}	degrees	at/g yr^{-1}	mm yr^{-1}	mm yr^{-1}	yr
VERM1	42.49926	3.13484	11495±9662	41	4.31	0.301± 0.257	0.346 ±0.296	2044
VERM2	42.49638	3.13239	8736±4224	42	4.30	0.395 ± 0.200	0.439 ± 0.222	1557
VERM3	42.49391	3.13232	31946±4775	46	4.29	0.108 ± 0.023	0.104 ± 0.022	5704
BRAV1	41.76295	2.99443	6855±1250	53	4.47	0.521 ± 0.123	0.393 ± 0.093	1182
BRAV2	41.76149	2.99260	10951±4014	45	4.43	0.324 ± 0.128	0.324 ± 0.128	1902
BRAV3	41.76090	2.98738	6301±1031	48	4.42	0.561 ± 0.125	0.505 ± 0.112	1097
BRAV4	41.75500	2.97478	8394±1936	55	4.42	0.421 ± 0.116	0.295 ± 0.081	1461
BRAV5	41.70699	2.89881	43646 ±3028	54	4.37	0.080 ± 0.013	0.058 ± 0.010	7670
COSTA1	-16.28077	-73.45072	5788±4044	39	2.55	0.376 ± 0.268	0.464 ± 0.331	1638
COSTA2	-16.24747	-73.54837	91661±5392	36	2.67	0.025 ± 0.004	0.034 ± 0.006	25010
COSTA3	-16.23203	-73.58788	132121±5214	34	2.92	0.018 ± 0.003	0.027 ± 0.004	33583
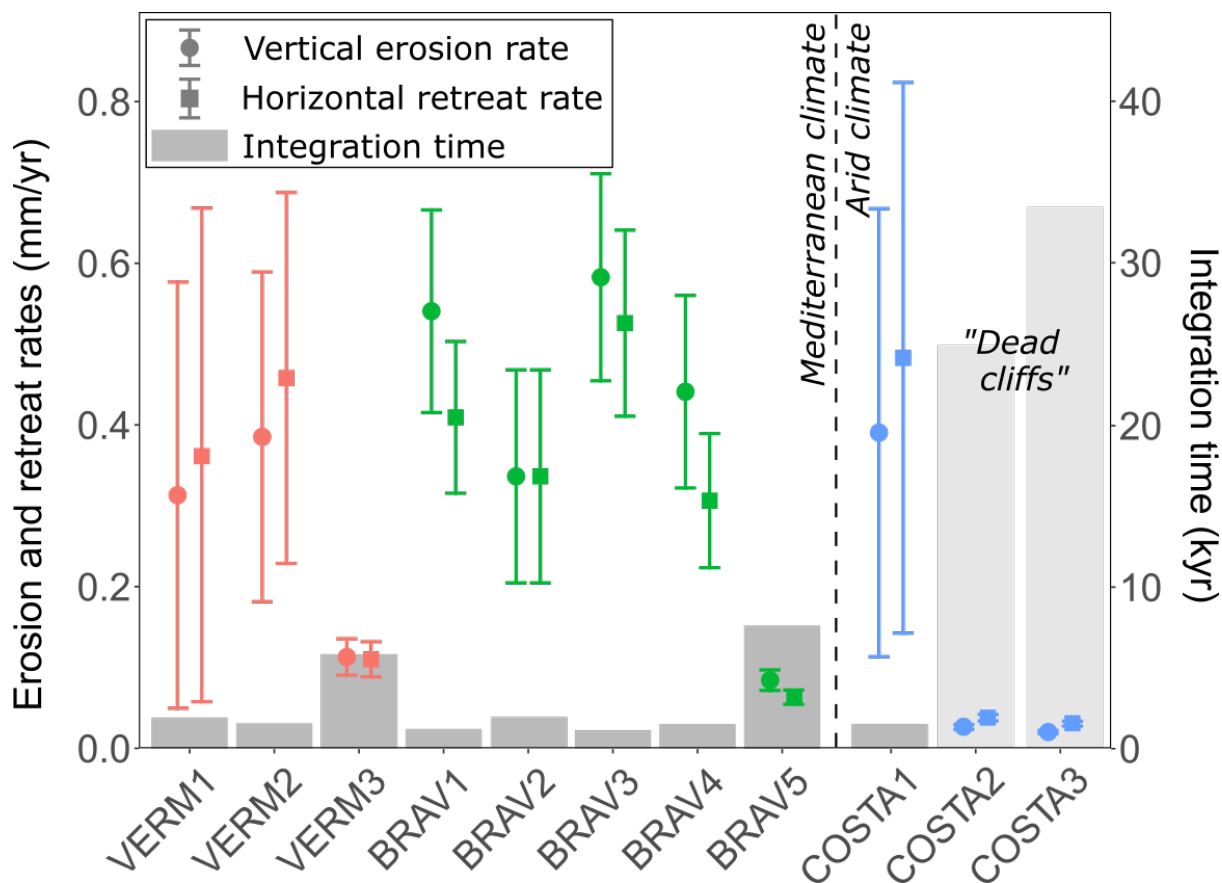
Figure 3. Results from the cosmogenic ^{10}Be abundance measurement in colluviums. Red: VERM series. Green: BRAV series. Blue: COSTA series. Circles: vertical erosion rates (ϵ) calculated from the C concentration of ^{10}Be. Squares: horizontal retreat rates (r) deduced from the mean cliff slope. Columns: integration time (τ) of the measurement. The colluviums at the VERM3 and BRAV5 sites are vegetated and the BRAV2 site is a cape, which is consistent with the lower erosion rates. Due to uplifted platforms at the base of the cliffs, coastal erosion no longer occurs on COSTA2 and COSTA3.

4 Discussion

The obtained erosion rates are remarkably consistent with their geomorphic setting. For the BRAV and VERM samples, six samples that could be considered as part of a repeatability test show similar erosion rates. The lower erosion rates of VERM3 and BRAV5 are consistent with the vegetated nature of colluvial wedges, either because the vegetation protects the coast from erosion or because lower erosion has allowed vegetation to develop.

The COSTA1 sample in Peru corresponds to an erosion rate similar to the values for the Mediterranean coasts, despite a more arid climate. It is beyond the scope of this paper to discuss the factors that control the coastal erosion in further depth, especially since it would require an analysis of the wave amplitude and frequency distribution. Nevertheless, the similar coastal erosion obtained in Peru and for the Mediterranean coast suggests that different combinations of climates, wave frequency distributions and vertical uplift rates may result in similar erosion rates.

Furthermore, the Peruvian site COSTA1 where waves attack the base of the cliff yields, as expected, presents a twenty times higher erosion rate than the other sites in front of uplifted marine terraces which are protected from wave action. One obvious limitation of our study is the lack of an alternative method for comparing the erosion values we obtain averaged over several millennia, which is often the case with any new method. We note, however, that the erosion rates of the two sites in Peru preserved from wave action (0.018-0.025 mm yr^{-1}) have values similar to the average erosion rates of the catchments draining the Andes near these sites (0.015-0.02 mm yr^{-1} - Starke et al., 2020). In the Pyrenees, the minimum erosion rates of the coastal escarpment (VERM3 and BRAV5) are similar to millennial erosion rates in the Pyrenees nearby (0.06-0.14 mm yr^{-1} - Molliex et al., 2016), as well as other small French catchments draining towards the Mediterranean in Southern Alps (Mariotti et al., 2021) and Corsica (Molliex et al., 2017) (0.01-0.24 mm yr^{-1}). However, these comparisons should be treated with caution as the erosion processes are different. Overall, the rates of cliff retreat are around 1 to 20 times higher than the average erosion rates in the nearby catchment areas.

As we have obtained coastal erosion values that are slower than those documented worldwide (Prémaillon et al., 2018), we discuss in the following several biases that could lead to an underestimation of retreat rates in our study.

One bias could be the contribution of grains eroded from the land surface above the rocky coast. Although we paid attention to select sites between rivers that ensure a negligible contribution of the land surface above the cliff, half of the surface of the catchment draining toward BRAV2 is on land. If the upstream zone erodes much more slowly than the coastal escarpment, it is possible that this contribution partly explains the slightly lower erosion rate of BRAV2. Nevertheless, even an extremely low erosion rate of the land surface above the coast could not decrease artificially the retreat rate by a factor larger than 1.5, because the contribution of this area to the flux of quartz grains would be negligible in that case (cf. Supplementary Material).

It has been shown that outcropping bedrock can erode at a smaller rate than surrounding loose material in a catchment (e.g Bierman and Caffee, 2001; Heimsath et al., 2006; Lodes et al., 2023). We may wonder if this difference can affect the estimation of the mean scarp erosion rate from the ^{10}Be concentration in colluvium. This is unlikely because the coastal scarp retreats horizontally, so that outcropping bedrock contributes as much as the other sources that provide the sampled colluvium over millennia. However, if a slower eroding part of the bedrock was not sampled at all by our approach, then our erosion rate would be overestimated, not underestimated. For the Peruvian samples, the coastal scarp is almost entirely covered by a regolith, so that the distinction between bedrock and loose sediment does not hold.

Another source of bias could be the shallow landslides that may feed the colluvium with grains that have lower ^{10}Be concentrations. However, in that case, the bias would increase the apparent erosion rate. Furthermore, the similar erosion rates obtained for five samples in the VERM and BRAV series in the same geomorphic context indicate that these stochastic processes have a negligible effect.

Another bias could arise from the delayed adjustment of the ^{10}Be concentration in response to an increase in the erosion rate. The coastal erosion rate probably increased once the current sea level had been established 6 kyrs ago in average (e.g Lambeck, 1997; Bintanja and van de Wal, 2008; García-Artola et al., 2018); this timescale is shorter than the integration time of samples VERM3 and BRAV5 . The cosmogenic signal adapts to a changing erosion rate with a delay. We thus wonder if the ^{10}Be signal could be inherited from a former low erosion rate period, leading to estimations of erosion rates smaller than one or two orders of magnitude. In order to quantify this bias, we carried out end-member simulations where the erosion rate is constant (0.05 or 0.5 mm yr^{-1}) during 100 kyrs and then multiplied by 10, 100 or 200 in the last 6 kyrs. In the worst scenario, the erosion rate averaged over the last 6 kyrs is underestimated by 80% (see Supplementary Material Figure S1). Therefore, this bias can reduce the real value by half but it cannot change the order of magnitude of these two erosion rates. In other words, if the retreat rate had been one or two orders of magnitude faster in the last 6 kyrs, the ^{10}Be concentration for VERM3 and BRAV5 should have recorded it. For the other samples subject to erosion by sea waves, the integration time is shorter than 6 kyrs, although the erosion rates are still low (< 1 mm yr^{-1}), which gives confidence in these low values.

5 Conclusions

Our approach provides a new method to quantify coastal erosion rates less than 1 cm yr^{-1} over millennia. These rates are typically averaged over integration periods of millennia, some of them (the highest integration times) encompassing the current highstand as well as the period beforehand when the sea level was lower and the waves did not reach the cliff foot. The bias on the coastal erosion rate associated with this variable erosion should not exceed -80%, thus giving a valuable order of magnitude for coastal retreat rates. As there is no limitation to reproduce this approach where colluvium is present, we anticipate that it will fill a significant gap in the rocky coast retreat rate database (retreat rates ranging 0.05-5 mm yr^{-1}), improve our understanding of controlling factors, as well as provide a temporal benchmark to evaluate current and future rocky coast erosion hazards.

Author contributions. Vincent Regard, Sébastien Carretier and Rémi Bossis designed the study, Rémi Bossis and Vincent Regard sampled the French sites, Sébastien Carretier sampled the Peruvian sites, Rémi Bossis, Sandrine Choy and Vincent Regard processed the samples, the manuscript was written collectively.

Competing interests. We declare no competing interests.

Data availability. The [10]Be raw data have been deposited on the Zenodo repository: https://doi.org/10.5281/zenodo.12750444. The DEM data can be found here for the French REG ALTI5 https://geoservices.ign.fr/ and here for the SRTM https://www.earthdata.nasa.gov/

Acknowledgements. The measurements were performed at the ASTER national accelerator mass spectrometry facility (CEREGE, Aix-en-Provence) that is supported by INSU/CNRS, ANR and IRD; we warmly thank ASTER Team (Georges Aumaître, Didier Bourlès (†), Karim Keddadouche). We are indebted to Sara Mullin for the English editing. This research was funded, in whole or in part, by ANR. A CC-BY public copyright license has been applied by the authors to the present document and will be applied to all subsequent versions up to the Author Accepted Manuscript arising from this submission, in accordance with the grant's open access conditions. We thank four previous reviewers, Klaus Wilcken and Luca Malatesta for their help in improving our manuscript.

References

Ashton, A., Walkden, M., and Dickson, M. E.: Equilibrium responses of cliffed coasts to changes in the rate of sea level rise, Marine Geology, 284, 217–229, https://doi.org/10.1016/j.margeo.2011.01.007, 2011.

Bierman, P. and Caffee, M.: Slow rates of rock surface erosion and sediment production across the Namib desert and escarpment, Southern Africa, American Journal of Science, 301, 326–358, 2001.

Bintanja, R. and van de Wal, R. S. W.: North American ice-sheet dynamics and the onset of 100,000-year glacial cycles, Nature, 454, 869–872, https://doi.org/10.1038/nature07158, 2008.

Braucher, R., Brown, E. T., Bourles, D. L., and Colin, F.: In situ produced Be-10 measurements at great depths: implications for production rates by fast muons, Earth And Planetary Science Letters, 211, 251–258, 2003.

Choi, K. H., Seong, Y. B., Jung, P. M., and Lee, S. Y.: Using Cosmogenic 10Be Dating to Unravel the Antiquity of a Rocky Shore Platform on the West Coast of Korea, Journal of Coastal Research, 282, 641–657, https://doi.org/10.2112/JCOASTRES-D-11-00087.1, 2012.

Clow, T., Willenbring, J. K., Young, A. P., Matsumoto, H., Hidy, A. J., and Shadrick, J. R.: Late Holocene Cliff Retreat in Del Mar, CA, Revealed From Shore Platform 10Be Concentrations and Numerical Modeling, Journal of Geophysical Research: Earth Surface, 128, e2022JF006 855, https://doi.org/10.1029/2022JF006855, 2023.

Cockburn, H., Brown, R., Summerfield, M., and Seidl, M.: Quantifying passive margin denudation and landscape development using a combined fission-track thermochronology and cosmogenic isotope analysis approach, Earth Planet. Sci. Lett., 179, 429–435, https://doi.org/10.1016/S0012-821X(00)00144-8, 2000.

Dewez, T., Rohmer, J., Regard, V., and Cnudde, C.: Probabilistic coastal cliff collapse hazard from repeated terrestrial laser surveys: case study from Mesnil Val (Normandy, northern France), In: Conley, D.C., Masselink, G., Russell, P.E. and O'Hare, T.J. (eds.), Proceedings 12th International Coastal Symposium (Plymouth, England), Journal of Coastal Research, Special Issue No. 65, 702–707, 2013.

DiBiase, R. A.: Increasing vertical attenuation length of cosmogenic nuclide production on steep slopes negates topographic shielding corrections for catchment erosion rates., Earth Surface Dynamics, 6, 2018.

Dornbusch, U., Robinson, D. A., Moses, C. A., and Williams, R. B. G.: Temporal and spatial variations of chalk cliff retreat in East Sussex, 1873 to 2001, Marine Geology, 249, 271–282, 2008.

Duguet, T., Duperret, A., Costa, S., Regard, V., and Maillet, G.: Coastal chalk cliff retreat rates during the Holocene, inferred from submarine platform morphology and cosmogenic exposure along the Normandy coast (NW France), Marine Geology, 433, 106 405, https://doi.org/10.1016/j.margeo.2020.106405, 2021.

García-Artola, A., Stéphan, P., Cearreta, A., Kopp, R. E., Khan, N. S., and Horton, B. P.: Holocene sea-level database from the Atlantic coast of Europe, Quaternary Science Reviews, 196, 177–192, https://doi.org/10.1016/j.quascirev.2018.07.031, 2018.

Hapke, C. J., Reid, D., and Richmond, B.: Rates and Trends of Coastal Change in California and the Regional Behavior of the Beach and Cliff System, Journal Of Coastal Research, 25, 603–615, 2009.

Heimsath, A. M., Chappell, J., Finkel, R. C., Fifield, K., and Alimanovic, A.: Escarpment erosion and landscape evolution in southeastern Australia, in: TECTONICS, CLIMATE, AND LANDSCAPE EVOLUTION, edited by Willett, S., Hovius, N., Brandon, M., and Fisher, D., vol. 398 of *Geological Society of America Special Papers*, pp. 173–190, https://doi.org/10.1130/2006.2398(10), geological-Society-of-America Penrose Conference, Taroko Natl Park, TAIWAN, JAN 13-17, 2003, 2006.

Hurst, M. D., Rood, D. H., Ellis, M. A., Anderson, R. S., and Dornbusch, U.: Recent acceleration in coastal cliff retreat rates on the south coast of Great Britain, Proceedings of the National Academy of Sciences, 113, 13 336–13 341, https://doi.org/10.1073/pnas.1613044113, 2016.

Lambeck, K.: Sea-Level change along the French Atlantic and Channel coasts since the time of the Last Glacial Maximum, Palaeogeog. Palaeoclim. Palaeoecol., 129, 1–22, 1997.

Letortu, P., Costa, S., Bensaid, A., Cador, J.-M., and Quénol, H.: Vitesses et modalités de recul des falaises crayeuses de Haute-Normandie (France) : méthodologie et variabilité du recul, Géomorphologie : relief, processus, environnement, 20, 133–144, https://doi.org/10.4000/geomorphologie.10588, 2014.

Lodes, E., Scherler, D., van Dongen, R., and Wittmann, H.: The story of a summit nucleus: hillslope boulders and their effect on erosional patterns and landscape morphology in the Chilean Coastal Cordillera, ESurf, 11, 305–324, https://doi.org/10.5194/esurf-11-305-2023, 2023.

Malatesta, L. C., Finnegan, N. J., Huppert, K. L., and Carreno, I, E.: The influence of rock uplift rate on the formation and preservation of individual marine terraces during multiple sea-level stands, Geology, 50, 101–105, https://doi.org/10.1130/G49245.1, 2022.

Mariotti, A., Blard, P.-H., Charreau, J., Toucanne, S., Jorry, S. J., Molliex, S., Bourles, D. L., Aumaitre, G., and Keddadouche, K.: Nonlinear forcing of climate on mountain denudation during glaciations, Nature GeoSciences, 14, 16+, https://doi.org/10.1038/s41561-020-00672-2, 2021.

Melnick, D.: Rise of the central Andean coast by earthquakes straddling the Moho, Nature Geosci, 9, 401–407, https://doi.org/10.1038/ngeo2683, 2016.

Molliex, S., Rabineau, M., Leroux, E., Bourles, D. L., Authemayou, C., Aslanian, D., Chauvet, F., Civet, F., and Jouet, G.: Multi-approach quantification of denudation rates in the Gulf of Lion source-to-sink system (SE France), Earth Planet. Sci. Lett., 444, 101–115, https://doi.org/10.1016/j.epsl.2016.03.043, 2016.

Molliex, S., Jouet, G., Freslon, N., Bourles, D. L., Authemayou, C., Moreau, J., and Rabineau, M.: Controls on Holocene denudation rates in mountainous environments under Mediterranean climate, EARTH SURFACE PROCESSES AND LANDFORMS, 42, 272–289, https://doi.org/10.1002/esp.3987, 2017.

Prémaillon, M., Regard, V., Dewez, T. J. B., and Auda, Y.: GlobR2C2 (Global Recession Rates of Coastal Cliffs): a global relational database to investigate coastal rocky cliff erosion rate variations, Earth Surface Dynamics, 6, 651–668, https://doi.org/https://doi.org/10.5194/esurf-6-651-2018, 2018.

Prémaillon, M., Dewez, T. J. B., Regard, V., Rosser, N. J., Carretier, S., and Guillen, L.: Conceptual model of fracture-limited sea cliff erosion: Erosion of the seaward tilted flyschs of Socoa, Basque Country, France, Earth Surface Processes and Landforms, 46, 2690–2709, https://doi.org/10.1002/esp.5201, 2021.

Regard, V., Saillard, M., Martinod, J., Audin, L., Carretier, S., Pedoja, K., Riquelme, R., Paredes, P., and Hérail, G.: Renewed uplift of the Central Andes Forearc revealed by coastal evolution during the Quaternary, Earth and Planetary Science Letters, 297, 199–210, https://doi.org/10.1016/j.epsl.2010.06.020, 2010.

Regard, V., Dewez, T., Bourlès, D. L., Anderson, R. S., Duperret, A., Costa, S., Leanni, L., Lasseur, E., Pedoja, K., and Maillet, G. M.: Late Holocene seacliff retreat recorded by 10Be profiles across a coastal platform: Theory and example from the English Channel, Quaternary Geochronology, 11, 87–97, https://doi.org/10.1016/j.quageo.2012.02.027, 2012.

Regard, V., Martinod, J., Saillard, M., Carretier, S., Leanni, L., Hérail, G., Audin, L., and Pedoja, K.: Late Miocene - Quaternary forearc uplift in southern Peru: new insights from 10Be dates and rocky coastal sequences, Journal of South American Earth Sciences, 109, 103 261, https://doi.org/10.1016/j.jsames.2021.103261, 2021.

320 Regard, V., Prémaillon, M., Dewez, T. J. B., Carretier, S., Jeandel, C., Godderis, Y., Bonnet, S., Schott, J., Pedoja, K., Martinod, J., Viers, J., and Fabre, S.: Rock coast erosion: An overlooked source of sediments to the ocean. Europe as an example, Earth and Planetary Science Letters, 579, 117 356, https://doi.org/10.1016/j.epsl.2021.117356, 2022.

Rogers, H. E., Swanson, T. W., and Stone, J. O.: Long-term shoreline retreat rates on Whidbey Island, Washington, USA, Quaternary Research, 78, 315–322, https://doi.org/10.1016/j.yqres.2012.06.001, 2012.

325 Rosser, N. J., Brain, M. J., Petley, D. N., Lim, M., and Norman, E. C.: Coastline retreat via progressive failure of rocky coastal cliffs, Geology, 41, 939–942, https://doi.org/10.1130/G34371.1, 2013.

Saillard, M., Audin, L., Rousset, B., Avouac, J.-P., Chlieh, M., Hall, S. R., Husson, L., and Farber, D. L.: From the seismic cycle to long-term deformation: linking seismic coupling and Quaternary coastal geomorphology along the Andean megathrust: Interseismic Coupling/- Coastal Morphology, Tectonics, 36, 241–256, https://doi.org/10.1002/2016TC004156, 2017.

330 Shadrick, J. R., Hurst, M. D., Piggott, M. D., Hebditch, B. G., Seal, A. J., Wilcken, K. M., and Rood, D. H.: Multi-objective optimisation of a rock coast evolution model with cosmogenic ^{10}Be analysis for the quantification of long-term cliff retreat rates, Earth Surface Dynamics, 9, 1505–1529, https://doi.org/10.5194/esurf-9-1505-2021, publisher: Copernicus GmbH, 2021.

Starke, J., Ehlers, T. A., and Schaller, M.: Latitudinal effect of vegetation on erosion rates identified along western South America, SCIENCE, 367, 1358+, https://doi.org/10.1126/science.aaz0840, 2020.

335 Stokes, M. F., Larsen, I. J., Goldberg, S. L., McCoy, S. W., Prince, P. P., and Perron, J. T.: The Erosional Signature of Drainage Divide Motion Along the Blue Ridge Escarpment, J. Geophys. Res. Earth Surface, 128, https://doi.org/10.1029/2022JF006757, 2023.

Stone, J.: Air pressure and cosmogenic isotope production, J. Geophys. Res., 105, 23 753–23 759, https://doi.org/ISI:000089895700027, 2000.

Sunamura, T.: Geomorphology of Rocky Coasts, John Wiley & Sons, Chichester, UK, 1992.

340 Swirad, Z. M. and Young, A. P.: Spatial and temporal trends in California coastal cliff retreat, GEOMORPHOLOGY, 412, https://doi.org/10.1016/j.geomorph.2022.108318, 2022.

Swirad, Z. M., Rosser, N. J., Brain, M. J., Rood, D. H., Hurst, M. D., Wilcken, K. M., and Barlow, J.: Cosmogenic exposure dating reveals limited long-term variability in erosion of a rocky coastline, Nat Commun, 11, 3804, https://doi.org/10.1038/s41467-020-17611-9, 2020.

Trenhaile, A. S.: Rock coasts, with particular emphasis on shore platforms, Geomorphology, 48, 7, 2002.

345 Vacchi, M., Joyse, K. M., Kopp, R. E., Marriner, N., Kaniewski, D., and Rovere, A.: Climate pacing of millennial sea-level change variability in the central and western Mediterranean, NATURE COMMUNICATIONS, 12, https://doi.org/10.1038/s41467-021-24250-1, 2021.

von Blanckenburg, F.: The control mechanisms of erosion and weathering at basin scale from cosmogenic nuclides in river sediment, Earth And Planetary Science Letters, 237, 462–479, 2005.

Wang, Y. and Willett, S. D.: Escarpment retreat rates derived from detrital cosmogenic nuclide concentrations, ESurf, 9, 1301–1322, 350 https://doi.org/10.5194/esurf-9-1301-2021, 2021.

Young, A. and Carilli, J.: Global distribution of coastal cliffs, Earth Surface Processes and Landforms, https://doi.org/10.1002/esp.4574, 2019.

Zavala, V., Carretier, S., Regard, V., Bonnet, S., Riquelme, R., and Choy, S.: Along-Stream Variations in Valley Flank Erosion Rates Measured Using [10] Be Concentrations in Colluvial Deposits From Canyons in the Atacama Desert, Geophysical Research Letters, 48, https://doi.org/10.1029/2020GL089961, 2021.